Zeitschrift: Helvetica Physica Acta
Band: 42 (1969)
Heft: 7-8

Artikel: 12C(n, n), (n, n') and (n, n') 3 reactions at 14.1 MeV
Autor: Grin, G.A. / Vaucher, B. / Alder, J.C.
DOI: https://doi.org/10.5169/seals-114104

$^{12}C(n, n)$, (n, n') and $(n, n')3\alpha$ Reactions at 14.1 MeV [1])

by **G. A. Grin** [2]), **B. Vaucher, J. C. Alder** and **C. Joseph**
Institute of Nuclear Physics, University of Lausanne [3])

(10. VI. 69)

Abstract. The $^{12}C(n, n)$, (n, n') and $(n, n')\,3\,\alpha$ reactions have been studied at 14.1 MeV by a time-of-flight method, with a scintillating scatterer.

The angular distributions and integrated cross sections were obtained for the following channels: $Q = 0$ (0^+) and -4.43 MeV (2^+) for angles greater than 50°; $Q = -7.66$ MeV (0^+) (8.5 ± 2 mb), -9.63 MeV (3^-) (62.5 ± 5 mb), -10.1 MeV (0^+ or 2^+) (maximum 55 mb) and -10.84 MeV (1^-) (13–17 mb) over the whole angular range; -11.82 MeV (2^-) (3–7 mb) for angles smaller than 60°.

At low scattered neutron energies a continuum was observed for which the cross section ($\approx$ 100 mb, including the scattering to the broad level at 10.1 MeV) and the angular distribution were determined.

1. Introduction

Elastic and inelastic scattering of 14 MeV neutrons from ^{12}C has been studied several times, mainly by time-of-flight. Angular distributions and integrated cross sections are fairly well known for $Q = 0$ (0^+) and -4.43 MeV (2^+), but not as well for $Q = -9.63$ (3^-) and especially -7.66 MeV (0^+). Three determinations, at 14.1 MeV, were made in the last few years at CHALK RIVER [1], GRENOBLE [2] and in this laboratory, in a first experiment referred to as *I* [3].

The few data about the excitation of higher levels were obtained with emulsions [4–7]. The 0^+ (or 2^+) level at 10.1 MeV is peculiar because of its 2.5 MeV width [8–10]. A particle continuum which could be connected with this broad level was found in several experiments: $^{12}C\,(n,n')$ [3], $^{12}C\,(p,p')$ [11], [12], $^{10}B\,(^3He,p\alpha\alpha\alpha)$ [13], $^{11}B\,(d,n)\,^{12}C^*$ [14], [15], $^{14}N\,(d,\alpha)\,^{12}C^*$ [16] and $^{9}Be\,(\alpha,n)\,^{12}C^*$ [17]. In most cases, however, the main part of the continuum could be explained by multiparticle processes. With $^{12}C + n$, the following sequential two-body processes can contribute: $^{12}C\,(n,\alpha)\,^{9}Be^* \rightarrow n' + 2\,\alpha$; $^{12}C\,(n,{}^{8}Be)\,^{5}He \rightarrow \alpha + n'$; as well as the simultaneous break-up $(^{13}C^*) \rightarrow 3\,\alpha + n'$. Nearly half ($\approx$ 230 mb) of the nonelastic cross section ($\approx$ 525 mb) corresponds to the $3\,\alpha + n'$ final state; $^{12}C^*$, except in the first 2^+ state, $^{9}Be^*$, ^{8}Be and ^{5}He are all particle-unstable (see Figure 1). The $^{12}C\,(n,n')\,3\alpha$ reactions, as a whole, were studied by emulsion [18], [5] and cloud chamber [6] techniques; emulsions were also used [19], [20] for $^{12}C\,(n,\alpha)\,^{9}Be^*$.

[1]) Work supported by the Swiss National Foundation for Scientific Research.

[2]) Presently at the Swiss Embassy in Washington, D.C.

[3]) Address: 19, rue César-Roux, CH-1005 Lausanne, Switzerland.

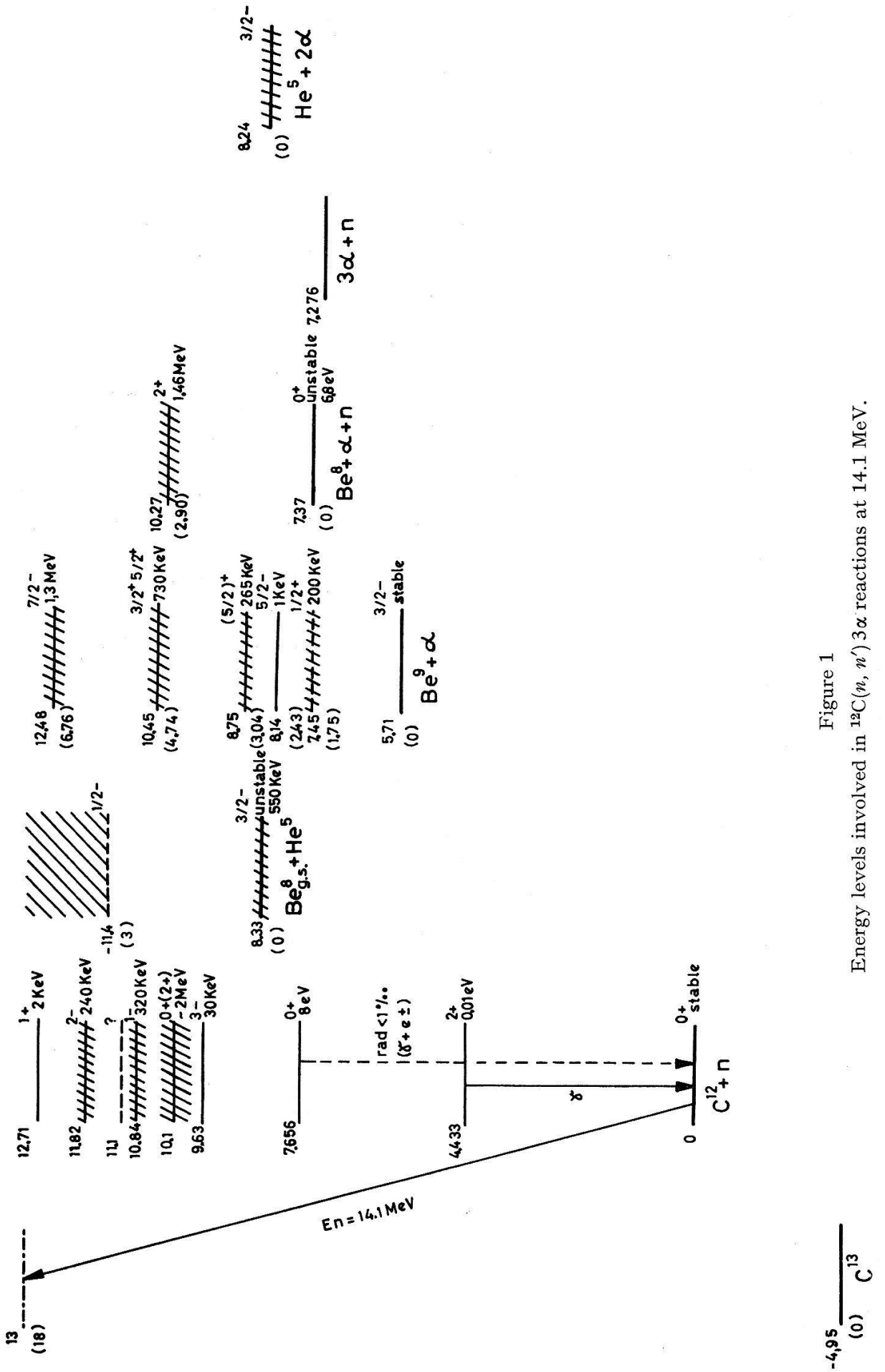

Figure 1

Energy levels involved in $^{12}C(n, n')\,3\alpha$ reactions at 14.1 MeV.

The corresponding proton induced reactions were also investigated: $^{12}C(p,p)$ and (p,p') at several energies between 14 and 19 MeV [11], [12]; $^{12}C(p,p'3\alpha)$ in the 15–29 MeV range [21].

We decided to make another time-of-flight experiment [22] regarding $^{12}C(n,n)$, (n,n') and $(n,n')3\alpha$ reactions at 14.1 MeV with an improved technique [23], to obtain more accurate cross sections for scattering to the 7.66, 9.63, 10.84 and 11.82 MeV states and to study the disputed broad level at 10.1 MeV.

2. Experimental Procedure

2.1 *The Method*

The carbon nuclei of an organic scintillator served as a scatterer. The neutron time-of-flight was recorded only when the associated event in the scatterer (carbon recoil or 3 α) had been detected in coincidence, after a pulse-height analysis [22], [23]. This reduced the number of random coincidences by a large factor (up to 20 compared with a graphite scatterer of the same size). Scattering by hydrogen in the scatterer, which could generally be distinguished, was used as a reference in the determination of the cross sections; it also showed the variation with energy of the neutron detector efficiency [22].

This method reduces the uncertainties in the measurement of absolute cross sections. The low light output of the organic scintillator for alpha particles and the even lower output for ^{12}C ions makes the detection of the associated events in the scatterer difficult; a 2 MeV ^{12}C ion, for example, produces the same pulse as a 30 keV electron only. The differences in light outputs, on the other hand, helps to discriminate between protons, alpha particles and ^{12}C ions [22], [23].

2.2 *Apparatus and Experimental Conditions*

The experiment was performed with a time-of-flight spectrometer of the associated-alpha-particle type [22].

The neutron detector consisted of a slab of plastic scintillator (NE 102A) $10\times10\times3.8$ cm viewed by a 56 AVP photomultiplier. The detection threshold was 500 keV proton energy (80 keV electron energy). Typical values of the intrinsic efficiency, measured as a function of the neutron energy, were 17.5% at 14.1 MeV, 22% at 7 MeV, 32% (maximum) at 2 MeV. A few measurements performed with another detector, which provided a $n-\gamma$ pulse-shape discrimination [24], gave the same results.

Two scintillating scatterers of different sizes were used, one for forward angles ($\leqslant 30°$), $1.8\times2.4\times2.8$ cm^3, the other for medium and backward angles, $3.0\times1.2\times4.8$ cm^3; each consisted of a NE 102A scintillator mounted on a 56 AVP photomultiplier and was placed at 15 cm from the neutron source. The angular resolution was 5° (fwhm). The measurements were performed in open geometry, with a shadow bar of iron 15 cm long only. The time resolution was 2 ns (fwhm), 5 ns (fw 10% m) for elastically scattered neutrons. The flight paths were 169 cm (0° to 90°) and 130 cm (90° to 150°).

The pulses from the scatterer were sorted according to their amplitude into three bands. By means of a multiple fast-slow coincidence-anticoincidence system, the

time-of-flight spectrum was divided into two simultaneously registered, partial spectra, each in 200 channels of a 400-channel pulse-height analyser. The lower band, gating the first spectrum, corresponded to '^{12}C' events, the middle one, gating the second spectrum, to '$3\,\alpha$' events; larger pulses, mainly due to proton recoils, were rejected, except during the reference measurements. The time intervals were measured by time-to-pulse-height conversion, with a three-diode circuit [25] and pentode limiters.

The nominal energy of the neutrons and the spread were 14.15 ± 0.05 MeV and 100 keV (fwhm), respectively. The neutron output was maintained at 10^7/sec, corresponding to $5 \cdot 10^4$ α/sec detected. Each measurement took between 30 and 60 hours.

2.3 *Evaluation of the Cross Sections*

The differential cross sections were evaluated taking the hydrogen data obtained with the same apparatus as a reference; the angular distribution (nearly isotropic in the CM system) and the integrated cross section (690 mb) are well known for np scattering at 14.1 MeV.

In the computation, multiple scattering (including the effective attenuation) in the scatterer was taken into account, assuming the same contribution of multiple scattered neutrons in 'H' and 'C' measurements.

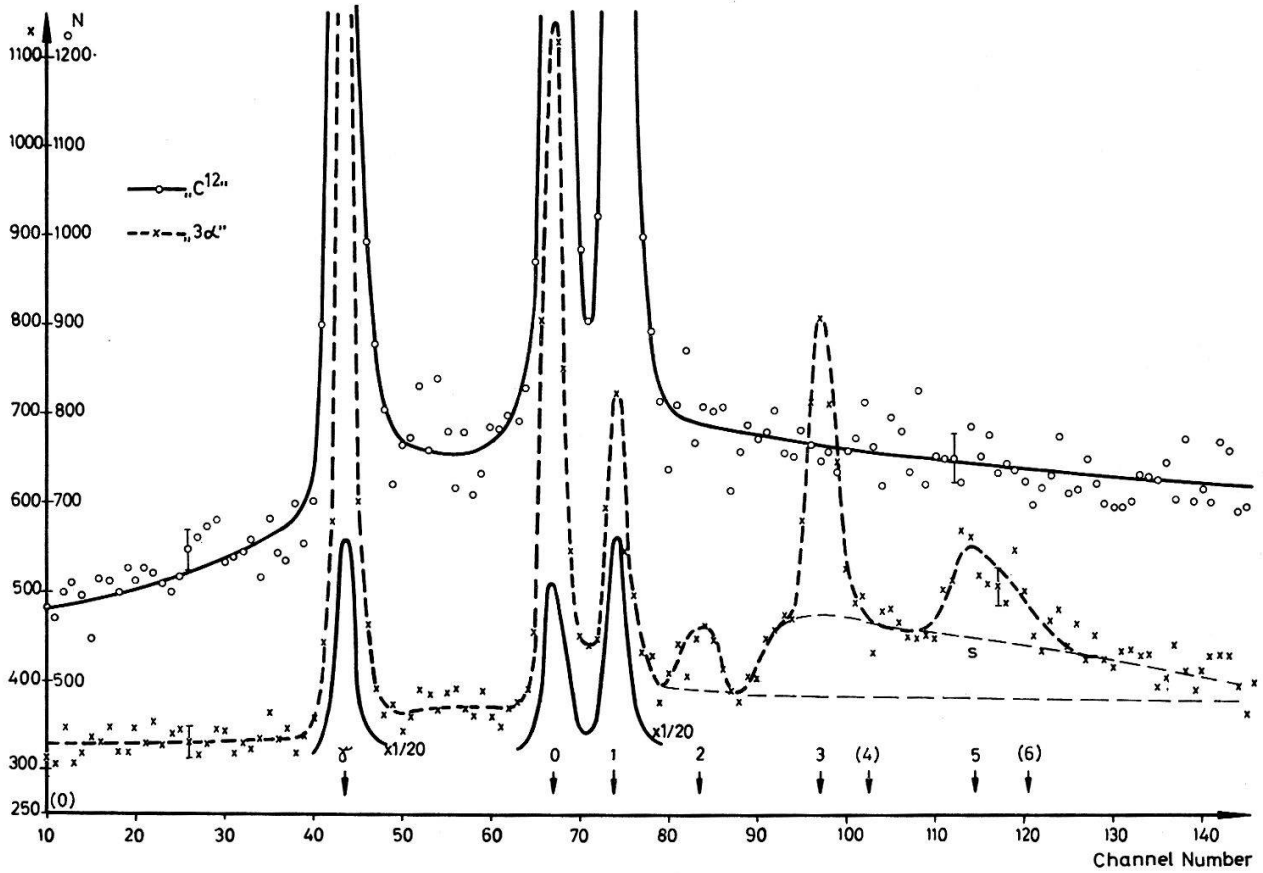

Figure 2

Double time-of-flight spectrum at $\theta_L = 135°$; flight path: 130 cm, duration: 50 hours. Time scale: 1.05 ns/channel. The calculated positions of the neutron groups are indicated by arrows; the numbers correspond to the $^{12}C^*$ levels; (0): ground state, (1): first excited state, ... (6): 11.1 MeV state.

It was necessary to draw a separation curve (S in Figures 2 and 6) between the continuum and the neutron groups corresponding to the scattering from the 9.63, 10.84 and 11.82 MeV levels, which are superposed on it in the time-of-flight (or energy) spectrum.

3. Results, Comparisons and Discussion

We give our results [22], [26], [27][4]) for the differential cross sections in Figures 3, 4 and 5[4]), with previous determinations and theoretical predictions. The errors include statistical and systematic contributions which come mostly from the background subtraction and occasionally from the distribution of the events between the various groups, including the continuum.

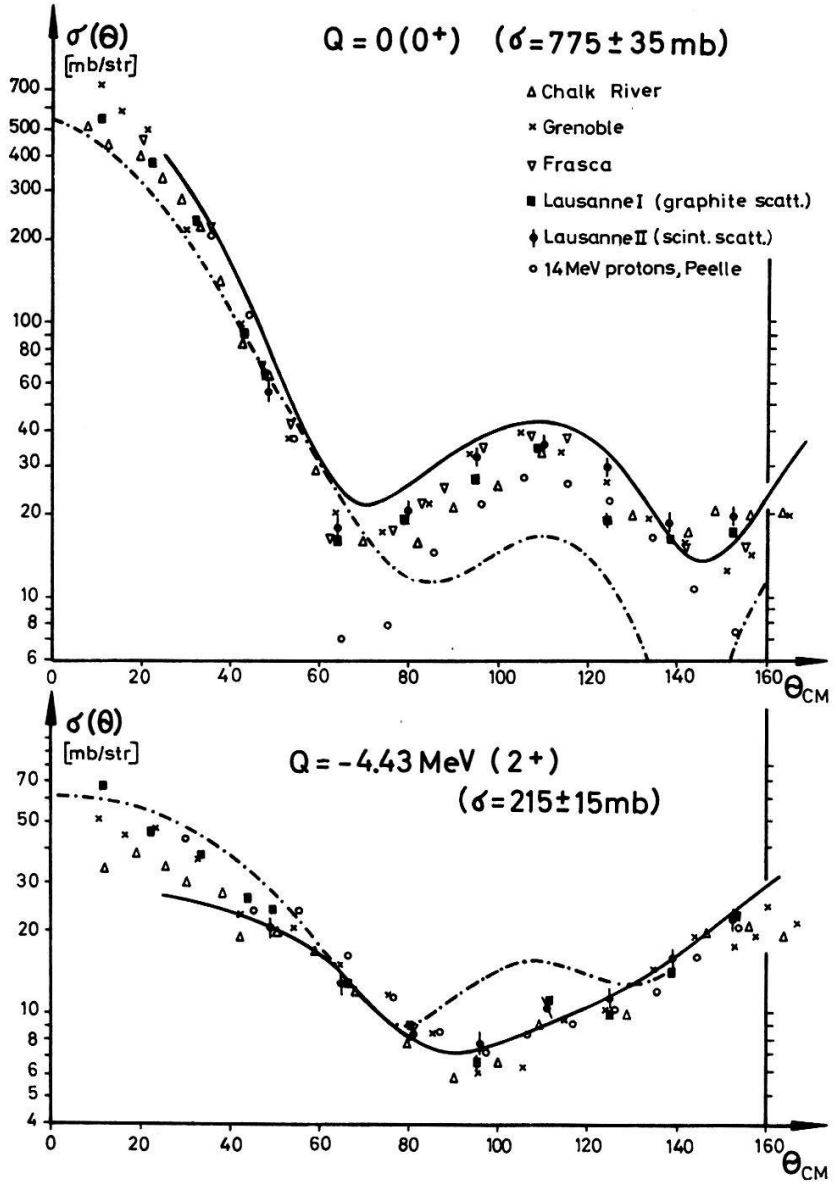

Figure 3

Experimental results for $Q = 0$ and $Q = -4.43$ MeV compared with previous ones. The curves are theoretical calculations obtained by: a) Tamura-Wong, coupled equations, $\beta_2 = -0.60$ (solid line), b) Bloore-Brenner, coupled equations, $V_{NN} = 78$ MeV (dash-dotted line).

[4]) Numerical tables may be obtained from Lausanne.

In a comprehensive theoretical calculation [27], Tamura and Wong used a collective-model coupled-channel formalism; apart from the effect of the permanent deformation of the nucleus ($\beta_2 = -0.60$), they considered other intrinsic and collective excitations. They obtained very good results for the elastic scattering and the scattering to the 2^+ (4.43 MeV), 3^- (9.63 MeV) and 1^- (10.84 MeV) states by coupling three channels together (0^+ 2^+ 3^-, 0^+ 2^+ 1^-). We do not show those results here as they have already been published [27] but we give (Fig. 3) some other unpublished results obtained by the same authors [28].

3.1 *Elastic Scattering and Excitation of the First Level*

We have only results for angles greater than 50° as far as the $Q = 0$ and $Q = -4.43$ MeV channels are concerned; at smaller angles, the carbon recoil energies were too small (< 0.6 MeV) to provide a 100%-efficient detection (in the scatterer). Our results are in good agreement with previous ones [1][5]), [2], [3], [29], especially with I; the results of the two experiments performed in our laboratory together bring improved accuracy.

Figure 3 also includes 14 MeV proton data [11], [12] and two pairs of theoretical curves obtained by coupled-channel calculations: for the first one [30] a microscopic description was used ($V_{NN} = 78$ MeV, Yukawa's shape); the second one shows a result Tamura and Wong obtained [28] by coupling two channels only; it is slightly different from the results mentioned before [27], but just as good.

3.2 *Inelastic Scattering from the 7.66 and 9.63 MeV Levels*

The various results [1–3], [26], [31] for scattering to the 0^+ and 3^- states do not agree as well as the above mentioned (Fig. 4). The disagreement is particularly important in the case of the 0^+ state. This is probably due to the difficulty of evaluation of the background, which is not only composed of random coincidences and which is relatively more important because of the small cross sections corresponding to this level.

We were careful to detect the low-energy (0.5 MeV for forward scattering) 3α events associated with the neutrons scattered from the 7.66 MeV level [22]. Further evidence for a complete detection could be seen in the fact that our cross sections for $Q = 0$ and -4.43 MeV agree with those of other authors for the case $E_{^{12}C} > 0.6$ MeV. It was not possible to determine the cross section around 45° (in the laboratory) because of the contamination from scattering on hydrogen at this angle; the contamination left is due to an imperfect pulse-height analysis on the scatterer; a 1% contamination corresponds to 1.5 mb/sr while the cross section to be measured is smaller than 1 mb/sr.

For $Q = -9.63$ MeV, the subtraction of the continuum on which the peak is superposed is the main cause of uncertainty. Peelle's results [11] for 16.7 MeV protons are also shown on Figure 4 since no data at 14 MeV exists. The behaviour of the proton cross sections for $Q = 0$, -4.43 and -9.63 MeV between 14 and 19 MeV [11], [12] and their comparison with neutron data at 14 MeV support the small cross sections we quote for $Q = -7.66$ MeV, which agree with the only three points obtained at CHALK RIVER [1].

[5]) For ref. [1] see also footnote [c]) of Table 1.

There is no satisfactory DWBA result for the $0^+ \rightarrow 0^+$ excitation[6]), which is difficult to describe whatever the model is. The coupled-channel formalism has not been applied successfully either [27]. For the $0^+ \rightarrow 3^-$ excitation, the situation is better. Figure 4 shows a curve resulting from a collective DWBA [33]; the fit yields a parameter $\beta_3 \approx 0.6$, which can be compared with $\beta_3 = 0.4$ from the analysis of 46 MeV proton scattering [32].

We have also included in Figure 4 the rather good results given by two simple models (for the shape of the angular distributions only, however): the diffraction

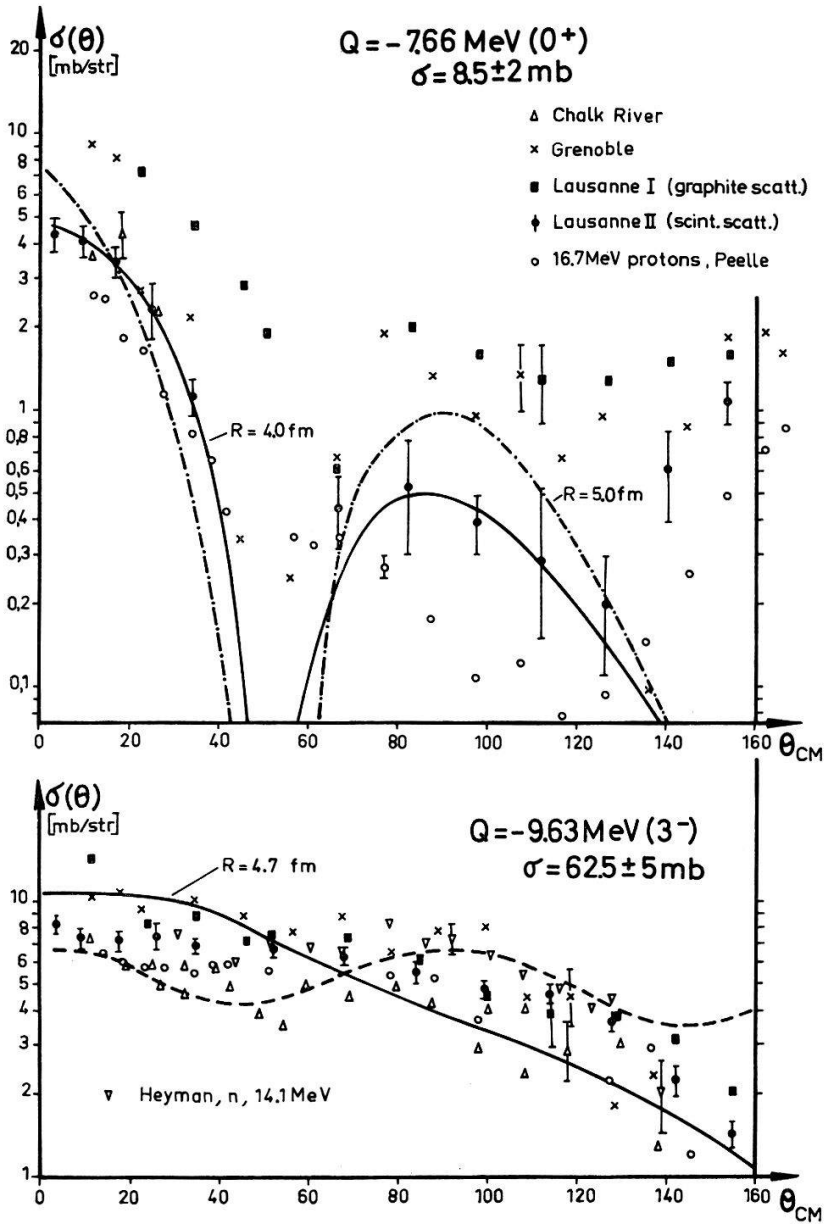

Figure 4

Experimental results for $Q = -7.66$ MeV and $Q = -9.63$ MeV. The curves correspond to theoretical calculations obtained from: a) Dar diffraction model, with indicated values of the interaction radius (solid line). b) Plane wave Born approximation for the $Q = -7.66$ MeV level (dash-dotted line). c) Clarke, collective DWBA, with $\beta_3 = 0.6$ (dashed line).

[6]) See, however, the analysis of 46 MeV proton scattering by SATCHLER [32], who assumes in particular a multiple excitation process through the 2^+.

model [34] for both levels and the PWBA for the 0^+ (it fails completely for the 3^-).

3.3 *Excitation of the 10.84 and 11.82 MeV Levels*

These levels are probably 1^- and 2^- [13] (or both 1^- [15], [32] or both 2^- [32]), with widths $\Gamma = \Gamma_\alpha$ of 320 and 240 keV [16], [35] for decay to $\alpha + {}^8Be_{g.s.}$ and $\alpha + {}^8Be_{2+}$, respectively.

Because of the width of these levels and of their overlap with the continuum, the results [22] (Fig. 5) are less accurate than for the lower states, especially for the $Q = -11.82$ MeV; in this case, moreover, we can give results only for angles smaller than 60° (CM), because of the neutron detection threshold. Our results do not agree, for both distributions, with those of the only other determination that we know of, an emulsion study [7]. There, the distributions are nearly isotropic – only four points were measured for each – with cross sections around 15 mb/sr.

Figure 5 also shows a collective-DWBA [33] curve for the 1^- level; from the fit a parameter $\beta_1 \approx 0.2$ (dipole vibration) can be extracted, but its significance is not clear. The result of the collective-model coupled-channel calculation can be seen in [27]. As far as the 2^- level is concerned, if the interaction is of a direct type, the transition $(0^+ \to 2^-)$ requires a spin-flip process or must be a multiple process [32].

The width of these two levels is enhanced by the expansion of the time scale at low neutron energies. Because of this we may have somewhat under estimated the values of the cross sections. They are likely to be closer to the upper limit given by the error margins in Figure 5. Again we can find some support from a proton study for the small cross sections we quote; from an energy spectrum given in [12], it can be deduced that the cross sections, for both levels, are indeed of the order of 2 mb/sr.

3.4 *Neutron Continuum. Excitation of the 10.1 MeV Level*

At low scattered neutron energies a continuum is clearly visible in each spectrum under the peak $Q = -9.63$ MeV and the bumps $Q = -10.84$ and -11.82 MeV (see Fig. 2 and 6). Its shape and place in the energy scale, in the CM system, do not change much with the scattering angle; lower energy neutrons are always more numerous. A comparison of the '^{12}C' and '$3\,\alpha$' spectra, for each angle, shows that the continuum cannot be explained by multiple scattering; this conclusion is supported by Monte-Carlo calculations [3].

Figure 5 shows two angular distributions for the whole continuum, with two different cut-offs for low neutron energies: a) the maximum excitation energy in $^{12}C^*$ is fixed at 11.8 MeV; b) the minimum neutron energy in the laboratory is fixed at 1 MeV. The integrated cross section, in either case, is large ($\approx$ 100 mb).

Three mechanisms can contribute to the continuum:

(i) *Scattering to a broad level around 10 MeV in* $^{12}C^*$.

To evaluate the maximum contribution of this mechanism, we followed an analysis previously made [17] for $^9Be(\alpha, n)^{12}C^*$. If we fit the maximum of the calculated spectrum q $(E_{n_{CM}})$, for a 0^+ level, to the observed continuum (curve S) around an excitation energy of 10 MeV (Fig. 6), we can explain 45–60% of it. The corresponding cross section is 55 ± 12 mb when the contribution is extrapolated to an excitation energy of 13 MeV. Such a large cross section would be surprising; this and the fact

that the angular distribution is not far from isotropy (Fig. 5) would appear to be more consistent with a 2^+ rather than a 0^+ assignment, in agreement with conclusions of Morinaga based on other considerations [36].

(ii) *$^{12}C(n,\alpha)^9Be^*$ and $^{12}C(n,^5He)^8Be$ reactions,* in which neutrons are emitted in the second or the third step of a sequential process. These reactions are not yet known well enough [19], [20], [35] to estimate their contributions. The $^{12}C(n,\alpha)^9Be^*_{2.43}$ channel is

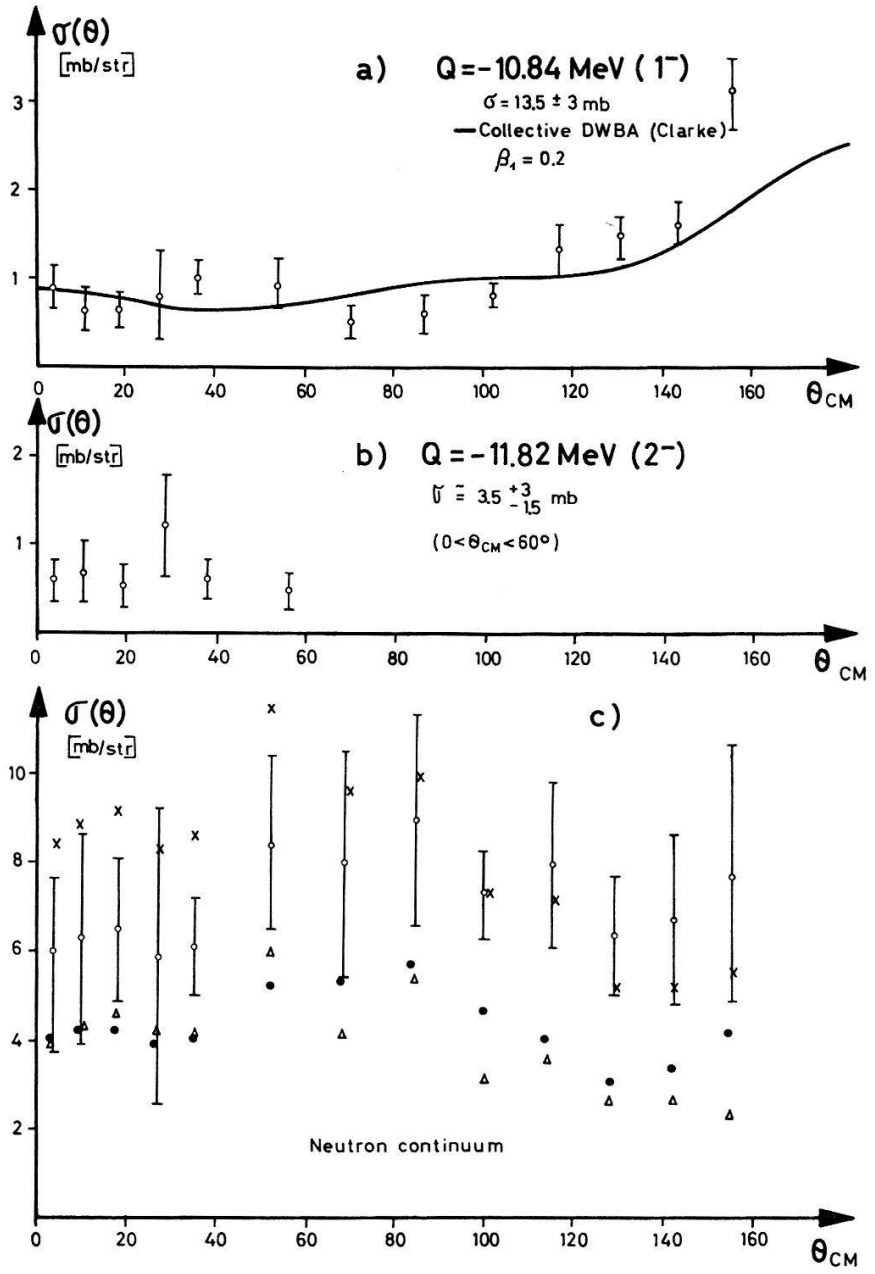

Figure 5

Experimental angular distributions. a) $Q = -10.84$ MeV (11.1 MeV included if it exists), with a DWBA curve. b) $Q = -11.82$ MeV. c) Neutron continuum: 1) Circles, with error bars: all events, with a 11.8-MeV limit on the maximum excitation energy in $^{12}C^*$ ($\sigma = 94 \pm 15$ mb). 2) Crosses (same relative errors as 1)): all events with a 1-MeV limit on the minimum neutron energy in the laboratory system ($\sigma = 102 \pm 15$ mb). 3) Dots (slightly larger relative errors than 1)): maximum possible contribution from scattering to the broad 10.1 MeV state (extrapolated limit: 13 MeV in $^{12}C^*$) ($\sigma = 55 \pm 12$ mb). 4) Triangles (slightly larger relative errors than 1)): remaining part of the continuum, 3) subtracted (limit: 1 MeV_n) ($\sigma = 45 \pm 10$ mb).

probably the most important ($\sigma \approx 50$ mb); the associated neutrons, however, have a maximum energy of 2.3 MeV, when emitted forward in the laboratory system, and 1.0 MeV, backward; they can therefore contribute to the low-energy part only of the continuum. Neutrons associated to $^{12}C(n, ^5He)^8Be$ would cover a broader spectrum, as would the neutrons resulting from the disintegration of $^9Be^*$ in states higher than the 2.43 MeV one [37].

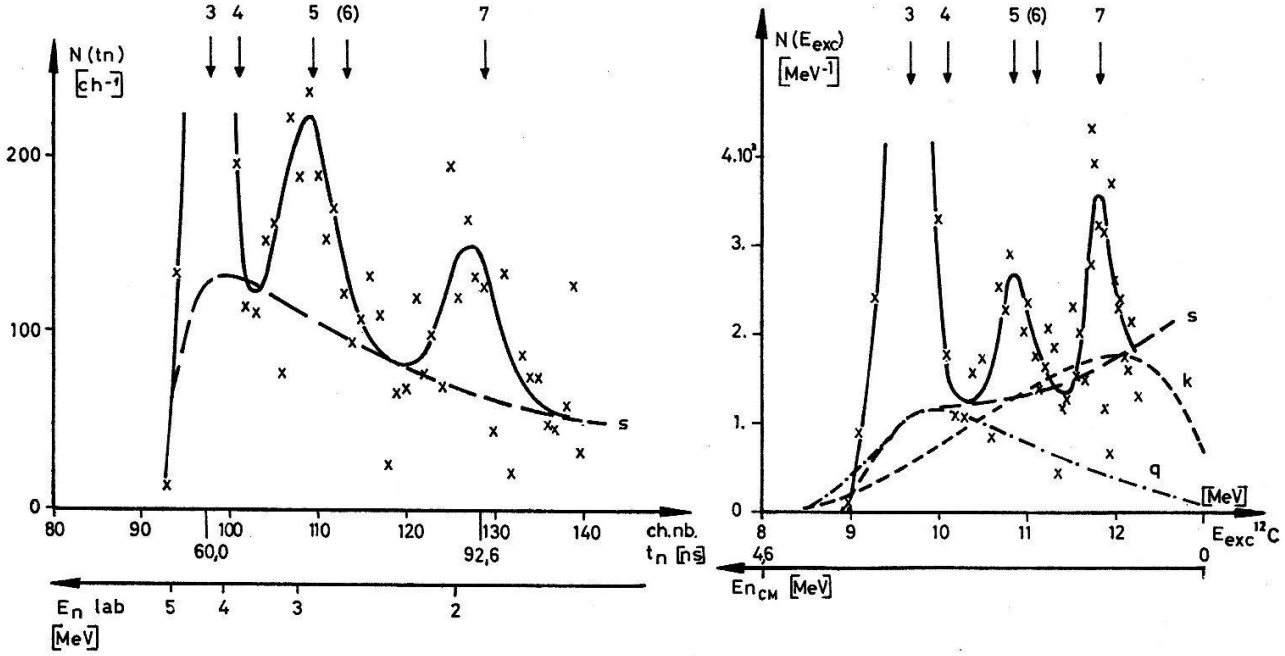

Figure 6

Time-of-flight and energy spectra of the part showing the continuum. 15°, 169 cm. The second one is obtained from the former by a conversion from time to neutron energy (lab.) scale, then to $^{12}C^*$ excitation energy scale, including the relative variation of the neutron detector efficiency. The curve s, k and q are defined in the text.

(iii) *Direct, simultaneous break-up* $(^{13}C^*) \rightarrow 3\alpha + n'$.

A phase-space distribution (curve k on Fig. 6), without correction, was also fitted to the whole continuum, explaining about 85% of it; 10 mb from the remainder could be attributed to scattering from the 10.1 MeV level. This repartition is not realistic, as it practically excludes mechanism (ii). A Maxwellian distribution (nuclear evaporation model) with a temperature of 1 MeV is close to the four-body phase-space.

In fact the situation might be intermediate, as found in the $^{12}C(p, p'3\alpha)$ case [21]: four-body break-up, but with some interaction between pairs, $(\alpha + \alpha)$ and $(\alpha + n)$ here. Moreover, scattering of 14 MeV neutrons from a particle-unbound level as broad as 2.5 MeV is not a simple two-body process; the times involved in the scattering and the disintegration processes are indeed of the same order.

3.5 *Integrated Cross Sections*

Some extrapolation was necessary, particularly towards 180° as usual, to get the integrated cross sections given by Table 1.

Table 1

	Integrated cross sections for scattering of 14.1 MeV neutrons from ^{12}C, in mb					idem with 16.7 MeV protons
[MeV]	Lausanne II	Lausanne I [a]	Grenoble [b]	Chalk River [c]	Others	Peelle [d]
Q = 0	(775 ± 35) [e]	770 ± 70	810 ± 80	730 ± 70	785 [f]	
−4.43	(215 ± 15) [e]	216 ± 25	215 ± 40	209 ± 20		
−7.66	8.5 ± 2	30 ± 15	16 ± 10		3-6 [g]	4.8 ± 0.2
−9.63	62.5 ± 5	72 ± 15	76 ± 13	45 ± 10	71 [h] 74 ± 10 [g]	51 ± 2
	Lausanne II	Brinkley [i]	Singletary [j]	Frye [k]	Mösner [g] (15.55 MeV)	
Q = −10.1	0-55					
−10.84	13-17	45 + 22			32 ± 6	
−11.1			124			
−11.82	3-7 [l]	34 ± 22			23 ± 8	
$\sigma^{inel}_{nn'3\alpha}$ [m]	115 ± 40 [n]	115 ± 45				
$\sigma_{nn'3\alpha}$ [o]	190 ± 20 [p]	(230 ± 50) [k]		230 ± 50	(316 ± 73) [k]	

a) Ref. [3].
b) Ref. [2].
c) Ref. [1]. In a recent paper [38], CLARKE and CROSS announced that the data they published in 1964 on C, Si and S and to which we referred had in fact to be multiplied by 1.08 ± 0.02. This is not done here, neither on the graphs.
d) Ref. [11].
e) Average values one may adopt taking into account the four (or five) determinations quoted here; the correction c) would increase them slightly, in particular the elastic cross section (≈ 785 mb).
f) Ref. [29].
g) Ref. [6]. Neutron energy: 15.55 MeV. The branching ratios were converted into cross sections by us, taking $\sigma_{nn'3\alpha} = 316 \pm 73$ mb.
h) Ref. [31].
i) Ref. [5]. Branching ratios converted into cross sections, with $\sigma_{nn'3\alpha} = 230 \pm 50$ mb (14.1 MeV).
j) Ref. [4].
k) Ref. [18].
l) For $0 < \theta_{C.M.} < 60°$ only.
m) Inelastic scattering only, $Q = -7.66$, -9.63, -10.1, -10.84, -11.82 MeV.
n) Taking 25 ± 25 mb for $Q = -10.1$ MeV.
o) All processes going to $3\alpha + n'$.
p) Bias on the laboratory neutron energy: 1 MeV.

A total cross section of 1.30 ± 0.01 b is a satisfactory value at 14.1 MeV. According to our results, the cross section for the processes our experiment does not cover (i.e. (n,α_0) and $(n,n'3\alpha)$ with $E_n < 1$ MeV) is therefore 120 ± 30 mb.

With regard to the data from other authors given in the table, we want to remark that BRINKLEY et al. [5] and MÖSNER et al. [6] only obtained branching ratios for the various channels and that they did not consider the possible excitation of the 10.1 MeV level; the last remark also applies to [7].

4. Conclusions

We have obtained results for $Q = 0$ and -4.43 MeV which are consistent with previous measurements. Our measurement gives more accurate results for the $Q = -7.66$ MeV and -9.63 MeV levels and new results concerning the $Q = -10.84$ and -11.82 MeV levels.

Moreover our measurements clearly showed an important continuum for which some useful information (shape, cross section, angular distribution) was obtained; however its precise origin is still uncertain because the $^{12}C\,(n,\alpha)\,^{9}Be^*$ and $^{12}C\,(n,{}^5He)\,^{8}Be$ reactions are not very well known. Half of the continuum at most can be attributed to inelastic scattering from the 0^+ (or 2^+) broad level around 10 MeV in $^{12}C^*$.

The results of several direct-interaction calculations, mostly with collective models, have been compared with the observed angular distributions. The coupled equations formalism once again proved to be valuable, except for the 0^+ state at 7.66 MeV. The collective character of the 2^+ (4.43 MeV), 3^- (9.63 MeV) and 1^- (10.84 MeV) states is confirmed. One also notices the surprising success of the diffraction model for $Q = -7.66$ MeV (0^+) and -9.63 MeV (3^-). But, in spite of this overall agreement, it would be desirable to have a satisfactory microscopic description of the interaction.

It thus appears that the elastic and inelastic scattering of 14 MeV neutrons from ^{12}C can be described as a direct process. The observed distributions, particularly their shape, cannot be explained by a compound-nucleus mechanism, except perhaps for the continuum; no narrow level has been observed so far near 18.0 MeV in $^{13}C^*$, the energy of the $^{12}C + n$ compound system at 14.1 MeV.

We wish to thank Professor CH. HAENNY for his interest and his support; Drs. T. TAMURA, C. Y. WONG and R. L. CLARKE for performing coupled-channel and DWBA calculations and kindly communicating their results; our colleagues J. F. LOUDE and Dr. A. HENCHOZ for their help in the electronics. We appreciate the helpful discussions we had with the late Dr. SAWICKI.

References

[1] R. L. CLARKE and W. G. CROSS, Nucl. Phys. *53*, 177 (1964).
[2] R. BOUCHEZ, J. DUCLOS and P. PERRIN, Nucl. Phys. *43*, 628 (1963). Int. Conf. on Fast Neutron Physics, Houston (1963). R. BOUCHEZ, private communication (1966).
[3] C. JOSEPH, G. A. GRIN, J. C. ALDER and B. VAUCHER, Helv. phys. Acta *40*, 693 (1967).
[4] J. B. SINGLETARY and D. E. WOOD, Phys. Rev. *114*, 1595 (1959).
[5] T. A. BRINKLEY, B. A. ROBSON and E. W. TITTERTON, Proc. Phys. Soc. *84*, 201 (1964).

[6] J. Mösner, G. Schmidt and J. Schintlmeister, Nucl. Phys. *75*, 113 (1966).
[7] M. Turk, Z. Naturf. *229*, 411 (1967).
[8] C. W. Cook, W. A. Fowler, C. C. Lauritsen and T. Lauritsen, Phys. Rev. *111*, 567 (1958).
[9] D. H. Wilkinson, D. E. Alburger, A. Gallmann and P. F. Donovan, Phys. Rev. *130*, 1953 (1963).
[10] D. Schwalm and P. Povh, Nucl. Phys. *89*, 401 (1966).
[11] R. W. Peelle, Phys. Rev. *105*, 1311 (1957).
[12] W. W. Daehnick and R. Sherr, Phys. Rev. *133*, B934 (1964).
[13] M. A. Waggoner, J. E. Etter, H. D. Holmgren and C. Moazed, Nucl. Phys. *88*, 81 (1966).
[14] W. C. Olsen, W. K. Dawson, G. C. Neilson and J. T. Sample, Nucl. Phys. *61*, 625 (1965). W. C. Olsen, private communication.
[15] H. Fuchs, K. Grabisch, P. Kraaz and G. Röschert, Nucl. Phys. [A] *105*, 590 (1967).
[16] W. A. Schier and C. P. Browne, Phys. Rev. *138*, B857 (1965).
[17] A. Nilsson and J. Kjellman, Nucl. Phys. *32*, 177 (1962); A. Nilsson, private communication.
[18] G. M. Frye, L. Rosen and L. Stewart, Phys. Rev. *99*, 1375 (1955).
[19] R. A. Al-Kital and R. A. Peck, Phys. Rev. *130*, 1500 (1963).
[20] M. L. Chatterjee and B. Sen, Nucl. Phys. *51*, 583 (1964).
[21] S. S. Vasilyev, V. V. Komarov and A. M. Popova, Nucl. Phys. *40*, 443 (1963).
[22] G. A. Grin, thèse, Lausanne (1967).
[23] G. A. Grin, C. Joseph, B. Vaucher, J. C. Alder, J. F. Loude and A. Henchoz, Helv. phys. Acta *38*, 666 (1965).
[24] A. Henchoz and C. Joseph, Helv. phys. Acta *38*, 663 (1965).
[25] G. A. Grin and C. Joseph, Nucl. Instr. *24*, 331 (1963).
[26] G. A. Grin, C. Joseph, J. C. Alder, B. Vaucher and J. F. Loude, Helv. phys. Acta *39*, 214 (1966).
[27] G. A. Grin, C. Joseph, C. Y. Wong and T. Tamura, Phys. Lett. *25 B*, 387 (1967).
[28] T. Tamura and C. Y. Wong, private communication.
[29] A. J. Frasca, R. W. Finlay, R. D. Koshel and R. L. Cassola, Phys. Rev. *144*, 854 (1966).
[30] F. J. Bloore and S. Brenner, Nucl. Phys. *69*, 320 (1965).
[31] M. Heyman, H. Jérémie, J. Kahane and R. Séné, J. Phys. *21*, 380 (1960).
[32] G. R. Satchler, Nucl. Phys. [A] *100*, 497 (1967).
[33] R. L. Clarke, private communication.
[34] A. Dar, Nucl. Phys. *55*, 305 (1964).
[35] F. Ajzenberg-Selove and T. Lauritsen, Nucl. Phys. *11*, 1 (1959); Nucl. Phys. [A] *114*, 1 (1968).
[36] H. Morinaga, Phys. Lett. *21*, 78 (1966).
[37] R. Barjon, Y. Flamant, J. Perchereau and A. Rode, Nucl. Phys. *36*, 247 (1962).
[38] R. L. Clarke and W. G. Cross, Nucl. Phys. [A] *95*, 320 (1967).